

EFFECT OF SEVERE PLASTIC DEFORMATION ON THE POROSITY CHARACTERISTICS OF Al-Zn-Mg-Cu PM ALLOY

J. Bidulská¹, R. Kočíško¹, R. Bidulský², M. Actis Grande², T. Donič³, M. Martikán³

¹ Department of Metals Forming, Faculty of Metallurgy, Technical University of Košice, Vysokoškolská 4, 04200 Košice, Slovakia

² Politecnico di Torino-Alessandria Campus, Viale T. Michel 5, 15100 Alessandria, Italy

³ Faculty of Mechanical Engineering, University of Žilina, Univerzitná 1, 01026 Žilina, Slovakia

Received 11.12.2009

Accepted 03.02.2010

Corresponding author: R. Bidulský, Tel.: +39-0131-229 232, Fax: +39-0131-229 399, E-mail address: robert.bidulsky@polito.it, Politecnico di Torino-Alessandria Campus, Viale T. Michel 5, 15100 Alessandria, Italy

Abstract

The aim of this work was to perform an analysis of severe plastic deformation on the porosity characteristics of aluminium PM alloy. The studied Al-Zn-Mg-Cu aluminium alloy was pressed in two different pressures 400 and 600 MPa; than three different processing conditions (debinding at 400 °C for 60 min, sintering in a vacuum furnace at 610 °C for 30 min and Equal Channel Angular Pressing - Back Pressure) were carried out. Densification behaviour of powder particles in the studied Al-Zn-Mg-Cu aluminium alloy is complicated due to the large surface area and associated oxide layers. Therefore, the first pass of Equal Channel Angular Pressing - Back Pressure only caused powder particles to slide against each other with little appreciable deformation of them. The morphology (mainly represented by f_{shape} and f_{circle}), distribution and dimension (mainly represented by D_{circle}) of pores have a significant effect on the mechanical behaviour of powder metallurgy materials. Pore diameters for all processes materials are in the range of 1 to 45 μm , however most of the pores diameter values D_{circle} are in the range of 2 to 10 μm . It could be expected that this large amount of small pores influences strongly both f_{shape} and f_{circle} . Pore profile irregularity, represented by morphological parameter f_{circle} , is in the range of 0.23 to 0.25 and depicts evolution of pores to a smooth contour that is more effective than to a circular form during sintering, so the highest value of f_{shape} (as a pore elongation is in the range of 0.5 to 0.6) was registered for sintered and Equal Channel Angular Pressed - Back Pressure specimen as well.

Keyword: aluminium alloy, SPD, ECAP-BP, FEM, porosity

1 Introduction

Nowadays, one widely employed route to consolidate the aluminium alloys is powder metallurgy (PM) technology. Conventional press-and-sinter PM is an exemplary net shape process and therefore offers inexpensive manufacturing [1-3].

The traditional process is to obtain the improvement of the mechanical properties of aluminium alloys through the precipitation of a finely dispersed second phase in the matrix. This is accomplished by a solution treatment of the material at a high temperature, followed by quenching. The second phase is then precipitated at room or elevated temperatures. For aluminium alloys this procedure is usually referred to as age hardening and it is also known as

precipitation hardening [4]. In the past decade, the research focused on the strengthening of Al alloys without any ageing treatment, via severe plastic deformation (SPD) [4-6]. Representing one of severe plastic deformation methods, Equal Channel Angular Pressing (ECAP) is rather effective for producing ultrafine-grained (UFG) metals with enhanced mechanical and processing properties inherent in various UFG materials [7, 8]. The ECAP process is a promising method that involves large shear plastic deformation in a deforming layer of a workpiece. The application of back-pressure leads to a suppressing of damage accumulation and closure of defects, while the absence of back-pressure leads to the development of defects due to severe plastic deformation [9]. Authors [10] report that conventional forming methods and heat treatment can determine a limit in the level of strength-plastic characteristics adequate to structural properties in aluminium alloys. Presented results underline that a combination of high strength and ductility of ultrafine polycrystalline metals prepared by severe plastic deformation is unique and it indeed represents a interesting case from the point of view of mechanical properties, as confirmed in [11, 12].

Most of the properties of PM materials are strongly related to porosity. The pores act as crack initiators and due to their presence distribution of stress is inhomogeneous across the cross section and leads to reduction of the effective load bearing area. Both the morphology and distribution of pores have a significant effect on the mechanical behaviour of PM materials. The effect of porosity on the mechanical properties depends on several factors such as the quantity of pores, their interconnection, size, morphology and distribution [13]. Moreover, also the chemical composition the lubricant used the die design and the sintering parameters (atmosphere, temperature and time) impact on the influence of pores onto the components' characteristics.

In order to evaluate powder behaviour in nanoscale, some new approaches are necessary [14], as well as mathematical and computer simulation [15-18].

The aim of this work was to perform an analysis of severe plastic deformation on the porosity characteristics of aluminium PM alloy.

2 Material and experimental methods

The material used in this experiment was an aluminium alloy ALUMIX 431 (Al-5.5 wt.% Zn-2.5 wt.% Mg- 1.6 wt.% Cu- 1.0 wt.% Wax) supplied by Ecka Granules – Metal Powder Technologies.

Specimens were obtained using a 2000 kN hydraulic press, applying two different pressures (400 and 600 MPa). Unnotched impact energy specimens $55 \times 10 \times 10 \text{ mm}^3$ (ISO 5754) were prepared. Specimens were debinded in a ventilated furnace (Nabertherm) at 400 °C for 60 min. Sintering was carried out in a vacuum furnace (TAV) at 610 °C for 30 min, with an applied cooling rate (post sintering) of 6 °C/s. The set-up of ECAP-BP for the produced PM materials consisted of a vertical entrance channel with a forward pressing plunger and a horizontal exit channel with a back plunger providing a constant back pressure during pressing. The die had a 90° angle with sharp corners and channels of $6 \times 6 \text{ mm}^2$ in the cross section. Specimens were then inserted in the entrance channel with graphite lubrication. A heating device was employed to heat the die to 250 °C, which was kept under control to $\pm 1 \text{ °C}$ through a thermocouple mounted close to the intersection of the channels. A back pressure of 100 MPa was used. The specimens were ECAPed-BP for 1 pass. The processing conditions are presented in **Table 1**.

The metallographic specimens were impregnated with resin under vacuum in order to avoid any pore distortion during polishing. The microstructural characterization was carried out on unetched specimens using an optical microscope LEICA MPEF4 equipped with an image

analyzer and SEM Jeol 7000F. Characterization was carried out at $\times 200$ on the minimum 10 different image fields; this way, over 2000 pores were recorded and processed by Leica Qwin image analysis system.

Table 1 The processing conditions for studied aluminium alloy

No	Pressure [MPa]	Processing conditions
1a	400	debinding
1b	600	debinding
2a	400	debinding, ECAP-BP
2b	600	debinding, ECAP-BP
3a	400	debinding, sintering, ECAP-BP
3b	600	debinding, sintering, ECAP-BP

The following parameters were measured individually for each pore to describe the dimensional and morphological characteristics, such as D_{circle} (the diameter of the equivalent circle that has the same area as the metallographic cross-section of the pore) and morphological characteristics f_{shape} and f_{circle} which reflect form of the pores. The measured values of f_{shape} and f_{circle} were all divided by a correction factor of 1.064 according to recommendation by authors [19]. The calculations of both parameters are reported as follows:

$$f_{\text{shape}} = \frac{D_{\min}}{D_{\max}} \quad [-] \quad (1)$$

where

D_{\min} [μm] the parameter representing minimum of Feret diameter;

D_{\max} [μm] the parameter representing maximum of Feret diameter;

and

$$f_{\text{circle}} = \frac{4 \cdot \pi \cdot A}{P^2} \quad [-] \quad (2)$$

where

A [μm^2] the area of the metallographic cross-section of the pore

P [μm] the perimeter of the metallographic cross-section of the pore.

Two dimensional plane-strain finite element simulations of ECAP-BP were performed using the commercial program Deform 2D. A workpiece was defined as a porous material with apparent density of 0.604; as well as an elasto-plastic material with Al 6062 database characteristics. The tools of press and ECAP equipment (the die and plunger) were assumed to be rigid materials and they were assigned of tool steel material characteristic, being much higher than those of deformed material. Porosity distribution of as-pressed workpiece was directly interpolated to ECAP-BP workpiece. Subsequently, the workpiece was ECAPed and the back pressure was applied through a back pressing ram by edge force of 100 MPa.

3 Experimental results and discussion

3.1 Sintering conditions

Liquid phase sintering consists of typical stages. During the heating stage, the penetration of the pressing contacts by the transient liquid eutectic phases results in a pronounced expansion within

a rather small temperature interval. During further heating, when the solidus temperature for the composition is exceeded, also persistent liquid phase is formed, resulting in fast shrinkage. Depending on the selected heating rate and sintering temperature, the ratio solid-liquid varies and also the shrinkage does. The very sensitive solid-liquid equilibrium results in tight requirements for the tolerable temperature interval. It is well-known that for an effective liquid phase sintering, a wetting liquid represents an essential requirement. Authors [20-22] suggested that the Al-CuAl₂ eutectic can wet Al₂O₃ at 600 °C. However, not even Mg additions to melt Al reduce the contact angle sufficiently to produce wetting. This is possibly the main reason why sintering Al-Zn-Mg-Cu aluminium alloys still can be considered not that easy. It should be noticed, that investigated microstructures present the regions with alloying elements with high chemical activity, e.g. Cu and Mg, **Figs. 1** and **2**.

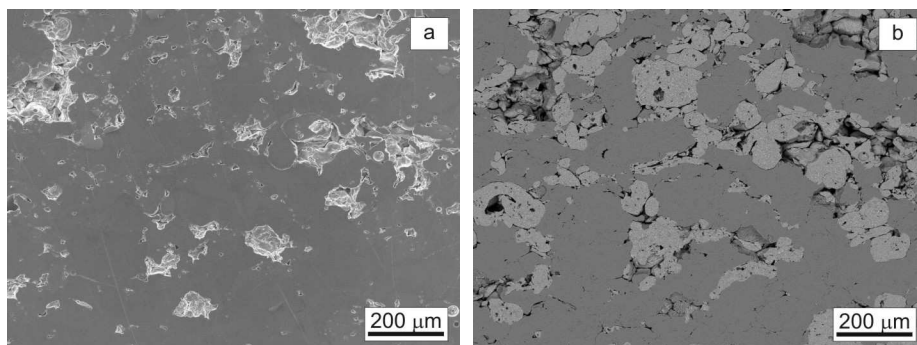


Fig.1 The typical microstructure for 400 MPa pressed specimens, a) SEI and b) COMPO

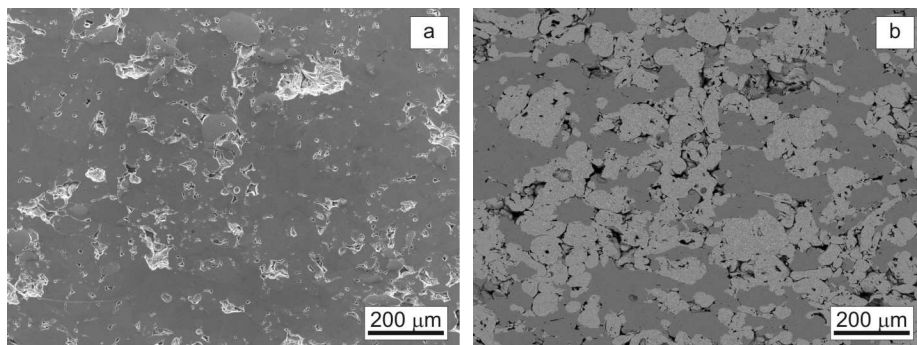


Fig.2 The typical microstructure for 600 MPa pressed specimens, a) SEI and b) COMPO

Mainly, Mg from the masteralloy particles is concentrated around the pores and in the necks volume. It appears that the primary porosity inside powder is also relatively permeable. The densification behaviour of powder particles in the examined alloy is complicated due to the large surface area and associated oxide layers. Therefore, the first pass of ECAP-BP only caused powder particles to slide against each other with little appreciable deformation of them; this is also confirmed in [23].

3.2 Consolidation processes

Consolidations of studied powder using FEM are illustrated in **Fig. 3** and **Fig. 4**.

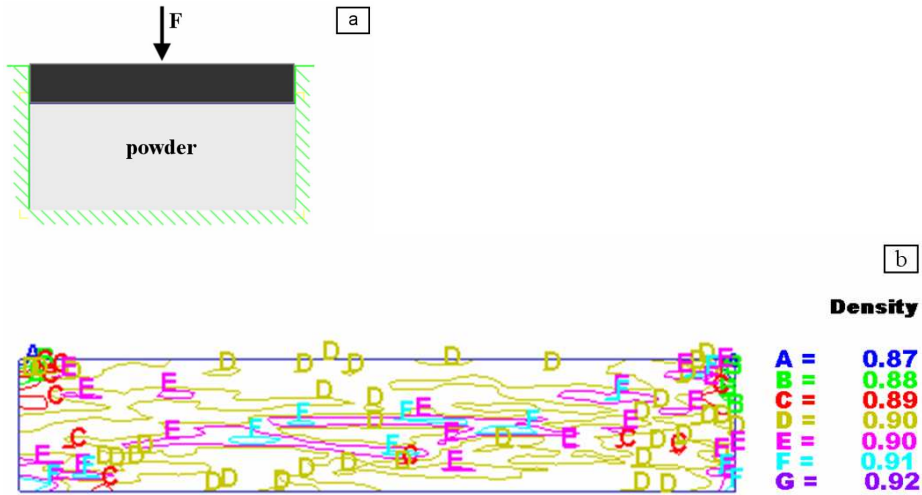


Fig.3 Consolidation of studied powder: a) powder; b) as-pressed



Fig.4 Porosity distribution after ECAP-BP

FEM analysis revealed that the workpiece is pressed through the die during ECAP; it undergoes severe plastic deformation within a region around the intersection plane of the two channels of the die (see the different relative density at the end of workpiece in Fig. 4). This region is affected by the plastic deformation zone (PDZ). The evolution of strain and its uniformity, as well as the resulting microstructure and material properties, depend on the characteristics of PDZ, as the distribution of strain rate. The porosity is located in particular in the bottom region of the workpiece close to the outer corner of the die, in the deformation areas called as tail, according to [24, 25]. The interaction of severe shear and the surface oxides, which are not disrupt neither during deformation nor in the processing (pressing, debinding and sintering) is therefore present in the component. Secondary porosity arises during liquid phase sintering. This is associated with wetting behaviour, swelling/shrinkage and particle size distribution as well as sintering processing conditions [26, 27].

Figs. 5-7 show the values of D_{circle} , f_{shape} and f_{circle} for the investigated material processed under the three different conditions considered. As expected, the sintering (coupled to SPD) tends to shift the distributions towards higher values of D_{circle} , f_{shape} , and f_{circle} ; the mean pore size is decreased and pore morphology is improved.

Application of ECAP-BP supported next decreasing of pore size, represented by the value of D_{circle} . It can be noted that most of the pores diameter values are around 2 to 10 μm in the whole amplitude, which ranged from 1 to 45 μm . It could be expected that this large amount of small pores strongly influences both f_{shape} and f_{circle} considering that small pores evolve easily to a circular form.

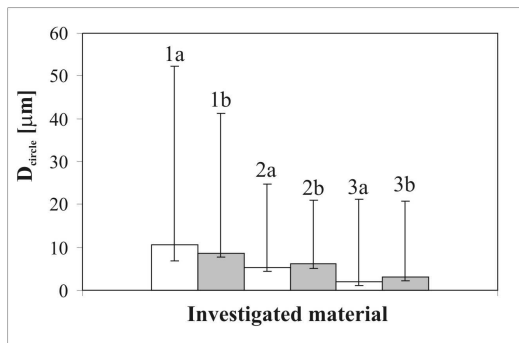


Fig.5 D_{circle} value for all the tested materials

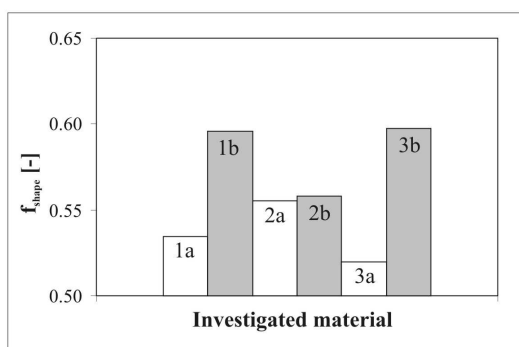


Fig.6 f_{shape} for all the investigated materials when considering the whole pore population

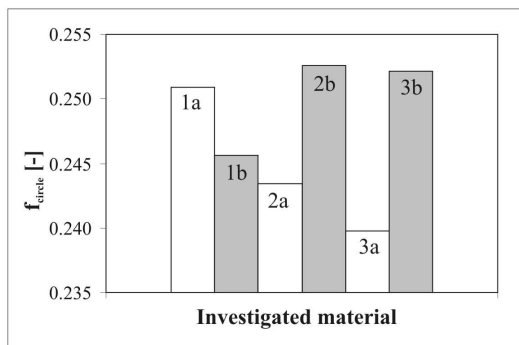


Fig.7 f_{circle} for all the investigated materials when considering the whole pore population.

The results presented in **Figs. 6** and **7** show a smaller value of f_{shape} approximately of 0.6 and f_{circle} approximately 0.25. Application of SPD process and sintering causes a decrease of D_{circle} to the minimum value of 2.08 for system 3a and, on the other hand, slightly increase the f_{circle} to maximum value of 0.6 for system 3b. It is interesting that, in terms of pressing pressure, the parameter D_{circle} has higher values for the initial state and the following processing causes contact areas between particles to increase and, consequently, a decrease in the effective shearing-stresses inside the particles. This condition happens with increasing densification, when

the powder particles are plastically deformed and increasingly deformation strengthened. Implementation of debinding process tends to generate larger pores in the microstructure, because of the lower densification attained on the green parts. When back pressure is applied, the stress distribution in deformed specimens causes the powder particles to squeeze together to such an extent that the initially interconnected pores transform to small isolated pores, determining a lower value of parameter D_{circle} . Consequently, ECAP-BP influences the porosity distribution in terms of the severe shear deformation involving and therefore influences the pore morphology which is represented by both parameters of f_{shape} and f_{circle} .

4 Conclusions

1. Pore diameters for all processes materials are in the range of 1 to 45 μm ; however most of the pores diameter values D_{circle} are in the range of 2 to 10 μm . It could be expected that this large amount of small pores influences strongly both f_{shape} and f_{circle} .
2. Pore profile irregularity, represented by morphological parameter f_{circle} , is in the range of 0.23 to 0.25 and depicts an evolution of pores to a smooth contour that is more effective than to a circular form during sintering, so the highest value of f_{shape} (as a pore elongation is in the range from 0.5 to 0.6) was registered for sintered and ECAPed-BP specimen as well.
3. ECAP-BP influences the porosity distribution in terms of the severe shear deformation involved and therefore influenced the pore morphology along with pore distribution.

Acknowledgements

This work is supported by Slovak Research and Development Agency - Bilateral Project SK-PL-0011-09. R. Bidulský thanks the Politecnico di Torino and the Regione Piemonte for co-funding by the fellowship.

References

- [1] R. Cook, I. T. H. Chang, C. L. Falticeanu: Materials Science Forum, Vol. 534-536, 2007, p. 773-776.
- [2] M. Hull: Powder Metallurgy, Vol. 40, 1997, No. 2, p. 102-103.
- [3] H. Danninger, H. C. Neubing, J. Gradl: *Sintering of High Strength Al-Zn-Mg-Cu Alloys to Controlled Dimensions*, In: PM'98 Granada, EPMA, Shrewsbury, Vol. 5, 1998, p. 272-277.
- [4] M. Fujda, M. Vojtko: Acta Metallurgica Slovaca, Vol. 13, 2007, SI., p. 585-591.
- [5] T. Kvačkaj, M. Fujda, O. Milkovič, M. Besterci: High Temperature Materials and Processes, Vol. 27, 2008, No. 3, p. 193-202.
- [6] J. Bidulská, T. Kvačkaj, R. Bidulský, M. Actis Grande: High Temperature Materials and Processes, Vol. 27, 2008, No. 3, p. 203-207.
- [7] M. Besterci, K. Sülleiová, T. Kvačkaj: Kovove Materialy, Vol. 46, 2008, No. 5, p. 309-311.
- [8] M. Besterci, T. Kvačkaj, L. Kováč, K. Sülleiová: Kovove Materialy, Vol. 44, 2006, No. 2, p. 101-106.
- [9] R. Y. Lapovok: Journal of Materials Science, Vol. 40, 2005, No. 2, p. 341-346.
- [10] J. Bidulská, T. Kvačkaj, R. Bidulský, M. Actis Grande: Kovove Materialy, Vol. 46, 2008, No. 6, p. 339-344.
- [11] R. Z. Valiev, R. K. Islamgaliev, I. V. Aleksandrov: Progress in Materials Science, Vol. 45, 2000, No. 2, p. 103-189.

- [12] R. Z. Valiev, T. G. Langdon: *Progress in Materials Science*, Vol. 51, 2006, No. 7, p. 881-981.
- [13] F. J. Esper, C. M. Sonsino: *Fatigue design for PM components*, EPMA, Shrewsbury, 1994.
- [14] E. Hryha, P. Zubko, E. Dudrová, L. Pešek, S. Bengtsson: *Journal of Materials Processing Technology*, Vol. 209, 2009, No. 5, p. 2377-2385.
- [15] R. Pernis: *Acta Metallurgica Slovaca*, Vol. 12, 2006, No. 1, p. 33-41.
- [16] R. Pernis, J. Kasala, J. Bořuta: *Acta Metallurgica Slovaca*, Vol. 15, 2009, No. 1, p. 5-14.
- [17] P. Baláž, T. Kvačkaj, M. Vlado, F. Ficek: *Acta Metallurgica Slovaca*, Vol. 11, 2005, SI. 2, p. 289-292, (in Slovak).
- [18] T. Kvačkaj et al.: *High Temperature Materials and Processes*, Vol. 26, 2007, No. 2, p. 147-150.
- [19] T. Marcu Puscas, M. Signorini, A. Molinari, G. Straffelini: *Materials Characterization*, Vol. 50, 2003, No. 1, p. 1-10.
- [20] S. W. Ip, M. Kucharski, J. M. Toguri: *Journal of Materials Science Letters*, Vol. 12, 1993, p. 1699-1702,
- [21] Y. Liu, Z. He, G. Dong, Q. Li: *Journal of Materials Science Letters*, Vol. 11, 1992, p. 896-898.
- [22] W. Kehl, H. F. Fischmeister: *Powder Metallurgy*, Vol. 23, 1980, No. 3, p. 113-119.
- [23] X. Wu, K. Xia: *Materials Science Forum*, Vol. 519-521, 2006, p. 1215-1220.
- [24] T. Kvačkaj et al.: *Kovove materialy*, Vol. 45, 2007, No. 5, p. 249-254.
- [25] J. Bidulská, R. Kočíško, T. Kvačkaj, R. Bidulský, M. Actis Grande: *Acta Metallurgica Slovaca*, Vol. 14, 2008, No. 3-4, p. 342-348.
- [26] J. Gradl, H. C. Neubing, A. Müller: *Improvement in the Sinterability of 7-xxx-based Aluminium Premix*, In.: *Euro PM 2004*, Eds. H. Danninger, R. Ratzl, Wien, Vol. 4, 2004, p. 15-21.
- [27] J. M. Martín, B. Navarcorena, I. Arribas, T. Gómez-Acebo, F. Castro: *Dimensional Changes and Secondary Porosity in Liquid Phase Sintered Al Alloys*, In.: *Euro PM 2004*, Eds. H. Danninger, R. Ratzl, Wien, Vol. 4, 2004, p. 46-53.